

# Supramolecular Enhancement of Aminoxy ORCA Contrast Agents

Hamilton Lee,<sup>a</sup> Jenica L. Lumata,<sup>a</sup> Michael A. Luzuriaga,<sup>a</sup> Candace E. Benjamin,<sup>a</sup> Olivia R. Brohlin,<sup>a</sup> Christopher R. Parish,<sup>b</sup> Steven O. Nielsen,<sup>a</sup> Lloyd L. Lumata<sup>b</sup> and Jeremiah J. Gassensmith<sup>a,c</sup> \*

Received 00th January 20xx,  
Accepted 00th January 20xx

DOI: 10.1039/x0xx00000x

**Many contrast agents for magnetic resonance imaging are based on gadolinium, however side effects limit their use in some patients. Organic radical contrast agents (ORCAs) are potential alternatives, but are reduced rapidly in physiological conditions and have low relaxivities as single molecule contrast agents. Herein, we use a supramolecular strategy where cucurbit[8]uril binds with nanomolar affinities to ORCAs and protects them against biological reductants to create a stable radical *in vivo*. We further overcame the weak contrast by conjugating this complex on the surface of a self-assembled biomacromolecule derived from the tobacco mosaic virus.**

Of the many spatially resolved biomedical imaging techniques available, magnetic resonance imaging (MRI) is of particular importance in modern medicine due to its non-invasive nature, potential for high spatial resolution, tissue penetration, and lack of ionizing radiation.<sup>1</sup> MRI relies on detecting the energy released over time by water protons returning to magnetic equilibrium after a radio frequency pulse has been applied. This relaxation rate—or relaxivity—is highly dependent on the chemical environment of the water. Since water intrinsically possesses low sensitivity to magnetic fields, contrast agents are used to increase the contrast between different features in the final image<sup>2-4</sup> with the majority of modern MRI contrast agents based on Gd<sup>3+</sup> complexes.<sup>5-7</sup> Although Gd has performed<sup>8-10</sup> remarkably in clinical settings, concerns about its toxicity,<sup>11-15</sup> especially for patients with impaired renal functionality, have catalyzed efforts to design alternatives to Gd and other metal-based MRI contrast agents. Several types of metal-free contrast agents have been investigated<sup>16-23</sup> with organic radical contrast agents (ORCAs) based on paramagnetic aminoxy moieties showing significant promise. Aminoxy ORCAs are distinguished by their compatibility with existing MRI techniques, enabling facile implementation in current clinical settings, and have low cytotoxicity and high biodegradability, reducing the potential for side effects.<sup>24, 25</sup> However, two major issues prevent aminoxy-based ORCAs from replacing traditional contrast agents based on Gd: (i) their single unpaired electron provides

weaker contrast compared to the seven unpaired electrons of Gd and (ii) they are reduced rapidly to MRI-silent hydroxylamines in physiological conditions by compounds including ascorbate, saccharides, and cysteine-rich proteins.<sup>24</sup>

Contrast issues in ORCAs have improved greatly in recent years by attaching them to polymeric or biomacromolecular nanoparticle systems<sup>26-42</sup> that both create high local concentrations of aminoxy moieties and decrease the diffusional and rotational motion of the attached ORCAs. Because rotational correlation time is inversely proportional to relaxivity, attaching contrast agents onto large macromolecules will—in general—improve their performance. On the other hand, sensitivity to reduction *in vivo* has been more difficult to address as the reduction-oxidation (REDOX) potentials of aminoxy radicals are such that they are quickly reduced in the high physiological concentrations of ascorbate. Strategies to overcome this have primarily focused on mitigating reduction by installing sterically hindered moieties around the aminoxy radical and incorporating aminoxy-containing molecules into macromolecular systems that shield the radical.<sup>43</sup> Problematically, creating more steric bulk may also preclude water from interacting with the free electron, which is detrimental to good contrast; consequently, synthetic strategies to prevent reductants from reacting with the aminoxy radical must conceptually titrate good shielding of the relatively large reductants while not greatly inhibiting access of water.

In this work, we utilize a supramolecular strategy to overcome ORCAs' poor relaxivity and high sensitivity toward reduction by fabricating a viral nanorod-based ORCA inclusion complex—specifically a pseudorotaxane—wherein the macrocycle cucurbit[8]uril (CB[8]) binds with nanomolar affinities to TEMPO moieties that have been conjugated onto the exterior surface of an anisotropic virus-like particle (VLP). We also show that this architecture is effective at shielding the radicals from reduction by ascorbate while still allowing the exchange of water and providing high contrast *in vivo*. These results indicate that shielding of aminoxy radicals with macrocycles is a promising strategy in the pursuit of a persistent ORCA viable for clinical applications.

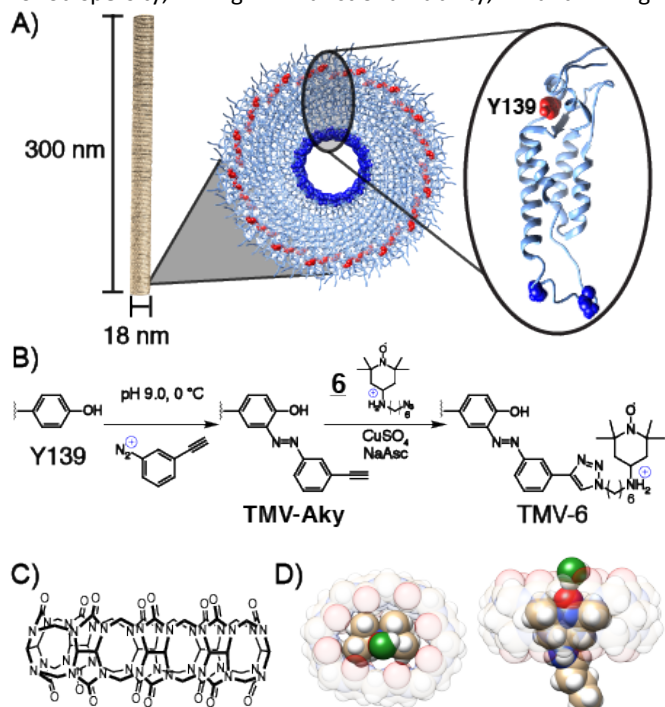
<sup>a</sup> Department of Chemistry and Biochemistry.

<sup>b</sup> Department of Physics.

<sup>c</sup> Department of Bioengineering, The University of Texas at Dallas, 800 West Campbell Rd. Richardson, TX 75080

Electronic Supplementary Information (ESI) available: [details of any supplementary information available should be included here]. See DOI: 10.1039/x0xx00000x

To achieve maximum contrast, many types of nanomaterials have been investigated for their potential as platforms for aminoxyl-based MRI contrast agents. Relative to silica, synthetic polymer, or metallic nanoparticles, VLPs offer the advantages of monodispersity, high functionalizability, and high



**Scheme 1.** (A) Structure of TMV highlighting the solvent exposed amino acid residues of a single coat protein. (B) Installation of alkyne functionality on Y139 via diazonium coupling followed by the conjugation of **6** via CuAAC. (C) Structural formula of CB[8]. (D) CB[8]⊃**6** inclusion complex showing the TEMPO oxygen is accessible by water (green) but still embedded within the macrocycle and protected from reduction.

biodegradability.<sup>44-50</sup> VLPs are self-assembled macromolecular structures composed of tens to thousands of individual protein subunits. The particular VLP utilized in this study is the tobacco mosaic virus (TMV), a 300 × 18 nm rod-shaped plant virus with a central 4 nm pore along its axis of symmetry. The ease of synthetic modification and its resilience under a wide range of temperatures, solvents, and pH values have allowed TMV to function as a versatile platform in VLP technology for applications involving biomedicine and stimulus-responsive materials. Each virus is composed of 2130 identical self-assembled 17.5 kDa coat proteins<sup>51-53</sup> (**Scheme 1**) of which, tyrosine 139 (Y139), located on the outer surface of the rod is solvent exposed and available for functionalization.<sup>54-57</sup> To this exposed residue, we planned to conjugate a derivative of the aminoxyl radical TEMPO, compound **6**, featuring an ammonium for enhanced binding of CB[8].

Various derivatives of TEMPO have been shown<sup>58-63</sup> to bind CB[8] and we predicted that the amine in **6** would offer enhanced binding through an extra ion-dipole interaction with the oxygens in the crown of the macrocycle. Molecular dynamics equilibrium and free energy simulations of the CB[8]⊃**6** inclusion complex establish the stability and precise location of TEMPO within the CB[8] cavity and quantify the accessibility to solvent water molecules of the TEMPO oxygen

radical (see SI). Through equilibrium, adaptive biasing force, and umbrella sampling simulations we computed the free energy to reversibly remove TEMPO from the CB[8] cavity (see Fig. S13). From these data the equilibrium position of the TEMPO ring is 0.85 Å above the plane of the CB[8] ring and centered within it. From equilibrium simulations we observe that water hydrogen atoms are found preferentially a distance of 2 Å from the TEMPO oxygen radical (see Fig. S14). On average, one water hydrogen atom is found within 2.6 Å of the TEMPO oxygen radical. A representative snapshot of the CB[8] and TEMPO molecules along with the water molecule containing this hydrogen atom is shown in **Scheme 1D** and **Figure S15**. Since this water molecule is surrounded by other solvent water molecules, the water exchange needed to generate the MRI contrast is readily apparent. Prior to the conjugation of **6** to TMV, the binding of **6** to CB[8] was probed via isothermal titration calorimetry (ITC) (**Figure S9**). The  $K_d$  value for the CB[8]⊃**6** complex was determined to be  $1.5 \pm 0.1 \times 10^{-8}$  M—this nanomolar affinity between **6** and CB[8] is on par with many antibody-substrate binding affinities. This suggests CB[8]⊃**6** should remain associated under concentrations and time scales relevant for MRI contrast agents in murine models.

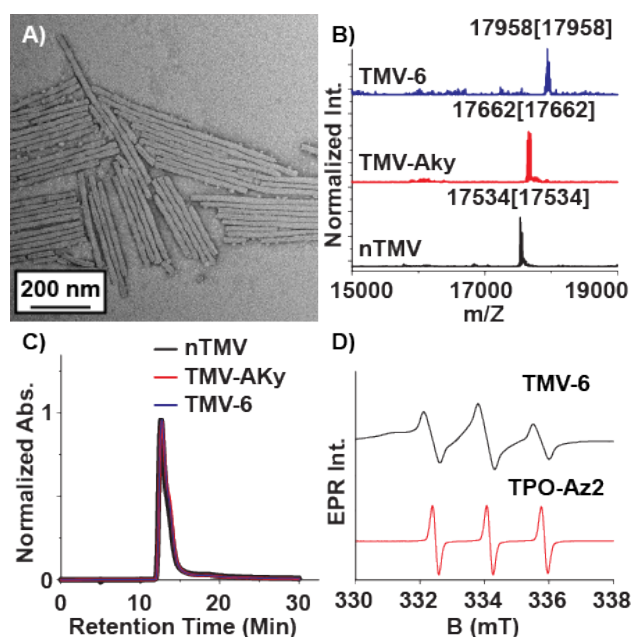


**Figure 1.** Characterization of TMV after bioconjugation reactions. (A) TEM image of TMV-6. (B) Bioconjugation of the TEMPO radical to TMV was confirmed via ESI-MS. The peak at 17534 m/z corresponds to native TMV. The peak at 17662 m/z corresponds to TMV-Aky. The peak at 17958 m/z corresponds to TMV-6. The spectrum corresponding to TMV-6 confirms complete conversion of TMV-Aky to TMV-6. (C) The integrity of the TMV rods after modification was confirmed by SEC. The single peak in the chromatograms (@260 nm) of the modified TMV samples demonstrates that the bioconjugation reactions did not compromise the morphology of the TMV rods. (D) X-band EPR spectra of **6** and TMV-6. The samples were prepared in capillary tubes to minimize interactions between high dielectric aqueous solvent and the electric field of the incident microwave radiation.

Compound **6** was attached to TMV by first conjugating an alkyne handle to Y139 (**Scheme 1**) via a diazonium coupling reaction to produce TMV-Aky. Following this, a copper-

catalyzed azide-alkyne cycloaddition (CuAAC) between TMV-Aky and **6** produced TMV-**6**. As seen in **Figure 1B**, ESI-MS confirmed quantitative conversions of the TMV coat proteins while TEM (**Figure 1A**) and SEC (**Figure 1C**) show that the size and morphology of the TMV rods were unaltered following bioconjugation. Finally, the EPR spectrum of the TMV-**6** conjugate (**Figure 1D**) shows a characteristic triplet centered at a  $g$ -value of 2.007 corresponding to  $^{14}\text{N}$  ( $I = 1$ ;  $A \sim 45$  MHz). The spectrum of **6** contains sharp peaks and isotropic  $g/A$  values that are characteristic of the rotational averaging found in small molecules. The spectrum of TMV-**6** contains broad peaks, anisotropic  $g/A$  values, and a lower S/N ratio relative to the spectrum of **6**. These differences between the spectra are attributed to the reduction of rotational and translational mobility upon attachment of **6** to the TMV rod. The high density of aminoxyl radicals on the surface of TMV can also allow for dipole spin exchange, which also results in peak broadening.

Since the properties of small molecules can change upon

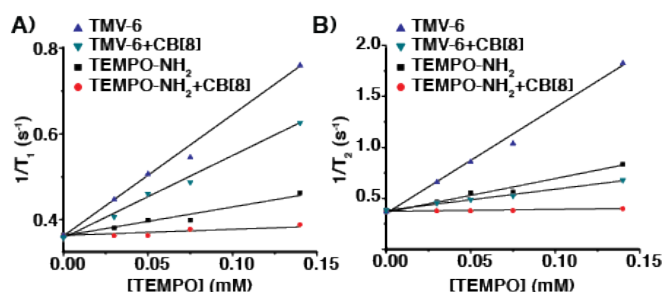


**Figure 2.** Plots of (A)  $1/T_1$  (s<sup>-1</sup>) and (B)  $1/T_2$  (s<sup>-1</sup>) versus [TEMPO] (mM) for TMV-**6** and compound **6** in the absence and presence of CB[8] at 43 MHz in KP buffer (0.1 M, pH 7.4) @ 310 K.

conjugation to proteins, we investigated the binding of CB[8] to TMV-**6** following the confirmation of the TMV-**6** conjugate. Since the solutions of TMV-**6** at concentrations required for ITC characterization were subject to viscosity and adhesion issues, a fluorescence titration was used instead to determine a dissociation constant. In this case, neither TMV-**6** nor CB[8] contain fluorophores, so a competitive binding strategy incorporating a fluorophore was implemented. Acridine-3,6-diamine, or Proflavin (PF), is an acridine derivative that is fluorescent as a free molecule in aqueous solutions, but its fluorescence becomes quenched<sup>64, 65</sup> upon binding inside the cavity of CB[8]. A fluorescence titration of increasing concentrations of TMV-**6** (0–20  $\mu\text{M}$  relative to TEMPO) titrated into solutions with a constant concentration of the CB[8] $\supset$ PF (0.2  $\mu\text{M}$ ) complex was performed. Upon the addition of increasing concentrations of TMV-**6**, the observed fluorescence of PF increased (**Figure S12**). Upon fitting these results (see Supporting Info) to the observed fluorescence intensities, the  $K_d$  value for the CB[8] $\supset$ TMV-**6** complex was determined to be  $3.8 \pm 0.5 \times 10^{-7}$  M. The reasons for the modest decrease in binding affinity of the CB[8] $\supset$ TMV-**6** complex relative to the CB[8] $\supset$ **6** complex is not yet fully known, but the binding is still high enough to be relevant for the purposes of the ORCA design. Taken as a whole, the fluorescence titration experiments suggest that CB[8] molecules can bind to the TEMPO moieties

conjugated onto the exterior surface of TMV to form a pseudorotaxane.

After establishing that CB[8] binds strongly to TMV-**6**, the relaxation behavior of the TEMPO moieties was evaluated to determine the suitability of the pseudorotaxane as an ORCA. Relaxation behavior is dependent on several factors, with magnetic field strength and solvent exchange being major examples. While maintaining a constant magnetic field strength of 1 T, longitudinal ( $T_1$ ) and transverse ( $T_2$ ) relaxation values were obtained for varying concentrations of TMV-**6** in the presence and absence of CB[8] (**Figure 2**). Relaxivity values ( $r_1$  and  $r_2$ ) were derived from a linear fit of the inverse relaxation data. When compared to the small molecule TEMPO control, the TMV-**6** conjugate exhibits higher  $r_1$  and  $r_2$  relaxivity values. This trend is observed for the comparison between TMV-**6** and free **6** when both are in the presence of CB[8]. The order of magnitude enhancements in relaxivity are expected and explained by the limited molecular motion provided by the attachment of TEMPO moieties to TMV. Upon the addition of CB[8], a reduction in  $r_1$  and  $r_2$  relaxivity values is observed for both TMV-**6** and the small molecule compound **6**. This reduction in relaxivity almost certainly occurs because of restriction of exchange of bulk water from the increased steric bulk of the CB[8]. The relaxivity values obtained by our experiments—which correlate with contrast strength—demonstrate that our pseudorotaxane provides the contrast required to function as an ORCA.

Having characterized the NMR relaxation properties of the

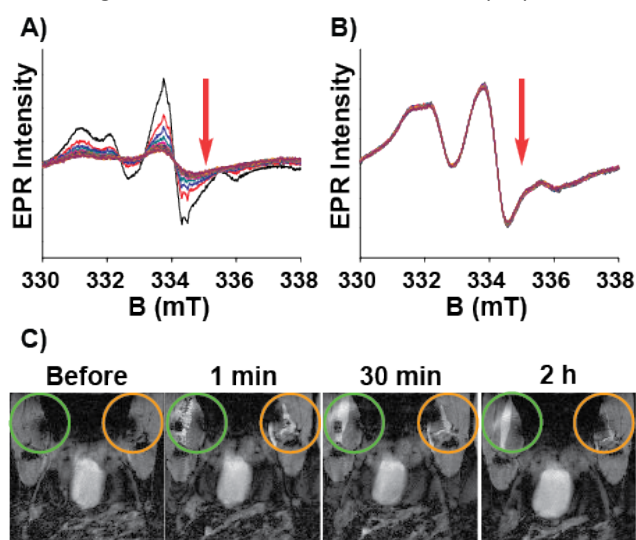


**Figure 3.** EPR spectra for the reduction of TMV-**6** (2.6 mg/mL) with sodium ascorbate (10 equivalents per TEMPO moiety) in the (A) absence and (B) presence of CB[8] (10 equivalents per TEMPO moiety). Data were collected at 10 min intervals over 2 h. (C)  $T_1$  weighted images of CB[8] $\supset$ TMV-**6** (green circle) vs TMV-**6** (orange circle) injected into the thigh muscle of a mouse.

pseudorotaxane and establishing its ability to function as an ORCA, we sought to investigate the shielding performance of the pseudorotaxane architecture. The rapid reduction of aminoxyl radicals to hydroxylamines in the presence of physiologically relevant reducing agents is well known.

Ascorbate is one example of these reducing agents and is commonly utilized for reduction experiments due to its ubiquity in the human body and its extensively studied redox properties. Upon the addition of a sodium ascorbate (10 equivalents per TEMPO moiety) solution in KP buffer (0.1 M, pH 7.4) to solutions of TMV-6 in the absence and presence of CB[8] (10 equivalents per TEMPO moiety), EPR spectra of the TMV conjugates were collected over 2 h (Figure 3). EPR intensities were fitted under pseudo-first-order conditions. The pseudo-first-order rate constant for the reduction of TEMPO,  $k'$ , was determined to be  $1.6 \pm 0.1 \times 10^{-3} \text{ s}^{-1}$  ( $t_{1/2} = 7.2 \text{ min}$ ) for TMV-6 in the absence of CB[8] and  $2.0 \pm 0.1 \times 10^{-5} \text{ s}^{-1}$  ( $t_{1/2} = 577.6 \text{ min}$ ) for TMV-6 in the presence of CB[8]. This two-order of magnitude rate reduction in the pseudorotaxane is far lower than that of—not only the unshielded TMV-6—but all aminoxyl-based ORCAs in the literature. The substantial decrease in the reduction rate of TEMPO suggests strongly that the CB[8] in the pseudorotaxane architecture effectively shields the aminoxyl radical from ascorbate.

We have demonstrated the enhancement of the survivability of aminoxyl radicals in the presence of ascorbate via shielding with CB[8]. The attachment of TEMPO derivatives onto the exterior surface of TMV results in a conjugate that provides enhanced  $T_1$  and  $T_2$  relaxation properties relative to small molecule aminoxyl radicals. The addition of CB[8] to the TMV conjugate forms a pseudorotaxane ORCA where the TEMPO moieties are encaged by CB[8]. The CB[8] can sterically shield the aminoxyl radical from reduction by ascorbate while still allowing for the exchange of water. Although the CB[8] also reduces the contrast strength of the ORCA compared to its unshielded form, the contrast strength is still higher than that of small molecule aminoxyl radicals. Furthermore, we were able to demonstrate the high contrast enhancement and stability of ORCA *in vivo* as shown in Figure 3C. We injected equal concentrations of CB[8]⊃TMV-6 (Figure 3 green circle) and TMV-6 (orange circle) into the thigh of a Balb/C mouse. Both probes initially showed bright contrast in the muscle; however, TMV-6 began to lose contrast quickly, with most signal gone after 2 h, in agreement with our EPR results. Most importantly, the ORCA can survive in the presence of ascorbate for periods of time that exceed—to the best of our knowledge (table S1)—currently known aminoxyl-based ORCAs by over two orders of magnitude.<sup>40-42, 66, 67</sup> Our results indicate that with the combined approach of (i) utilizing macrocycles for steric shielding to inhibit reduction *in vivo* along with (ii) enhancing  $T_1$  relaxivity by conjugating these supramolecular agents to biomacromolecular scaffolds, ORCAs are moving closer to clinically viable contrast agents.

## Conflicts of interest

There are no conflicts to declare.

## Funding

J.J.G would like to thank the National Science Foundation [CAREER DMR- 1654405] and the Welch Foundation [AT-1989-20190330]. C.E.B thanks the National Science Foundation Graduate Research Fellows Program (1746053). L.L.L would like to thank the Welch Foundation [AT-1877-20180324]. S.O.N. acknowledges that this project was partially funded by the University of Texas at Dallas Office of Research through the COBRA program.

## Notes and references

1. W.-Y. Huang and J. J. Davis, *Dalton Trans.*, 2011, **40**, 6087.
2. P. Caravan, *Chem. Soc. Rev.*, 2006, **35**, 512.
3. S. A. Corr, S. J. Byrne, R. Tekoriute, C. J. Meledandri, D. F. Brougham, M. Lynch, C. Kerskens, L. O'Dwyer and Y. K. Gun'ko, *J. Am. Chem. Soc.*, 2008, **130**, 4214-4215.
4. G.-L. Davies, S. A. Corr, C. J. Meledandri, L. Briode, D. F. Brougham and Y. K. Gun'ko, *ChemPhysChem*, 2011, **12**, 772-776.
5. P. Caravan, J. J. Ellison, T. J. McMurry and R. B. Lauffer, *Chem. Rev.*, 1999, **99**, 2293-2352.
6. E. J. Werner, A. Datta, C. J. Jocher and K. N. Raymond, *Angew. Chem. Int. Ed.*, 2008, **47**, 8568-8580.
7. P. Hermann, J. Kotek, V. Kubicek and I. Lukes, *Dalton Trans.*, 2008, DOI: 10.1039/b719704g, 3027.
8. Z. Zhou and Z.-R. Lu, *Wiley Interdisciplinary Reviews: Nanomedicine and Nanobiotechnology*, 2012, **5**, 1-18.
9. Y. Li, M. Beija, S. Laurent, L. v. Elst, R. N. Muller, H. T. T. Duong, A. B. Lowe, T. P. Davis and C. Boyer, *Macromolecules*, 2012, **45**, 4196-4204.
10. G.-L. Davies, I. Kramberger and J. J. Davis, *Chem. Commun.*, 2013, **49**, 9704.
11. I. A. Mendichovszky, S. D. Marks, C. M. Simcock and O. E. Olsen, *Pediatric Radiology*, 2007, **38**, 489-496.
12. F. G. Shellock and E. Kanal, *J. Mag. Res. Im.*, 1999, **10**, 477-484.
13. S. Swaminathan, T. D. Horn, D. Pellowski, S. Abul-Ezz, J. A. Bornhorst, S. Viswamitra and S. V. Shah, *N. Engl. J. Med.*, 2007, **357**, 720-722.
14. T.-H. Shin, Y. Choi, S. Kim and J. Cheon, *Chem. Soc. Rev.*, 2015, **44**, 4501-4516.
15. P. Verwilst, S. Park, B. Yoon and J. S. Kim, *Chem. Soc. Rev.*, 2015, **44**, 1791-1806.
16. E. Terreno, D. D. Castelli, A. Viale and S. Aime, *Chem. Rev.*, 2010, **110**, 3019-3042.
17. K. Glunde, D. Artemov, M.-F. Penet, M. A. Jacobs and Z. M. Bhujwala, *Chem. Rev.*, 2010, **110**, 3043-3059.
18. B. R. Smith and S. S. Gambhir, *Chem. Rev.*, 2017, **117**, 901-986.
19. P. Harvey, I. Kuprov and D. Parker, *Eur. J. Inorg. Chem.*, 2012, **2012**, 2015-2022.
20. N. R. B. Boase, I. Blakey and K. J. Thurecht, *Polymer Chemistry*, 2012, **3**, 1384.
21. I. Tirotta, V. Dichiarante, C. Pigliacelli, G. Cavallo, G. Terraneo, F. B. Bombelli, P. Metrangolo and G. Resnati, *Chem. Rev.*, 2015, **115**, 1106-1129.
22. S. Aime, D. D. Castelli, S. G. Crich, E. Gianolio and E. Terreno, *Acc. Chem. Res.*, 2009, **42**, 822-831.
23. G. Liu, X. Song, K. W. Y. Chan and M. T. McMahon, *NMR Biomed.*, 2013, **26**, 810-828.
24. J. T. Paletta, M. Pink, B. Foley, S. Rajca and A. Rajca, *Organic Letters*, 2012, **14**, 5322-5325.
25. Y. Wang, J. T. Paletta, K. Berg, E. Reinhart, S. Rajca and A. Rajca, *Org. Lett.*, 2014, **16**, 5298-5300.
26. E. A. Anderson, S. Isaacman, D. S. Peabody, E. Y. Wang, J. W. Canary and K. Kirshenbaum, *Nano Lett.*, 2006, **6**, 1160-1164.
27. A. Datta, J. M. Hooker, M. Botta, M. B. Francis, S. Aime and K. N. Raymond, *J. Am. Chem. Soc.*, 2008, **130**, 2546-2552.
28. M. A. Bruckman, L. N. Randolph, N. M. Gulati, P. L. Stewart and N. F. Steinmetz, *Journal of Materials Chemistry B*, 2015, **3**, 7503-7510.
29. N. Bye, O. E. Hutt, T. M. Hinton, D. P. Acharya, L. J. Waddington, B. A. Moffat, D. K. Wright, H. X. Wang, X. Mulet and B. W. Muir, *Langmuir*, 2014, **30**, 8898-8906.
30. H. Hu, Y. Zhang, S. Shukla, Y. Gu, X. Yu and N. F. Steinmetz, *ACS Nano*, 2017, **11**, 9249-9258.
31. M. A. Bruckman, S. Hern, K. Jiang, C. A. Flask, X. Yu and N. F. Steinmetz, *Journal of Materials Chemistry B*, 2013, **1**, 1482.
32. M. A. Bruckman, K. Jiang, E. J. Simpson, L. N. Randolph, L. G. Luyt, X. Yu and N. F. Steinmetz, *Nano Lett.*, 2014, **14**, 1551-1558.

33. J. Prasuhn, Duane E., R. M. Yeh, A. Obenaus, M. Manchester and M. G. Finn, *Chem. Commun.*, 2007, DOI: 10.1039/B615084E, 1269-1271.
34. L. Liepold, S. Anderson, D. Willits, L. Oltrogge, J. A. Frank, T. Douglas and M. Young, *Magnetic Resonance in Medicine*, 2007, **58**, 871-879.
35. P. D. Garimella, A. Datta, D. W. Romanini, K. N. Raymond and M. B. Francis, *J. Am. Chem. Soc.*, 2011, **133**, 14704-14709.
36. J. M. Hooker, A. Datta, M. Botta, K. N. Raymond and M. B. Francis, *Nano Lett.*, 2007, **7**, 2207-2210.
37. K. N. Raymond and V. C. Pierre, *Bioconjugate Chem.*, 2005, **16**, 3-8.
38. M. Allen, J. W. M. Bulte, L. Liepold, G. Basu, H. A. Zywicke, J. A. Frank, M. Young and T. Douglas, *Magnetic Resonance in Medicine*, 2005, **54**, 807-812.
39. S. Qazi, L. O. Liepold, M. J. Abedin, B. Johnson, P. Prevelige, J. A. Frank and T. Douglas, *Mol. Pharm.*, 2013, **10**, 11-17.
40. M. Dharmarwardana, A. F. Martins, Z. Chen, P. M. Palacios, C. M. Nowak, R. P. Welch, S. Li, M. A. Luzuriaga, L. Bleris, B. S. Pierce, A. D. Sherry and J. J. Gassensmith, *Mol. Pharm.*, 2018, **15**, 2973-2983.
41. A. O. Burtis, Y. Li, A. V. Zhukhovitskiy, P. R. Patel, R. H. Grubbs, M. F. Ottaviani, N. J. Turro and J. A. Johnson, *Macromolecules*, 2012, **45**, 8310-8318.
42. M. A. Sowers, J. R. McCombs, Y. Wang, J. T. Paletta, S. W. Morton, E. C. Dreaden, M. D. Boska, M. F. Ottaviani, P. T. Hammond, A. Rajca and J. A. Johnson, *Nature Communications*, 2014, **5**, 5460.
43. A. Rajca, Y. Wang, M. Boska, J. T. Paletta, A. Olankitwanit, M. A. Swanson, D. G. Mitchell, S. S. Eaton, G. R. Eaton and S. Rajca, *Journal of the American Chemical Society*, 2012, **134**, 15724-15727.
44. J. K. Pokorski, K. Breitenkamp, L. O. Liepold, S. Qazi and M. G. Finn, *J. Am. Chem. Soc.*, 2011, **133**, 9242-9245.
45. A. M. Wen and N. F. Steinmetz, *Chem. Soc. Rev.*, 2016, **45**, 4074-4126.
46. Z. Chen, Li, N., Li, S., Dharmarwardana, M., Schlimme, A., Gassensmith, J. J., *WIREs Nanomed. Nanobiotechnol.*, 2016, **8**, 512-534.
47. I. Yildiz, S. Shukla and N. F. Steinmetz, *Curr. Opin. Biotechnol.*, 2011, **22**, 901-908.
48. K. J. Koudelka, A. S. Pitek, M. Manchester and N. F. Steinmetz, *Annu. Rev. Virol.*, 2015, **2**, 379-401.
49. K. L. Lee, Shukla, S., Wu, M., Ayat, N. R., El Sanadi, C. E., Wen, A. M., Edelbrock, J. F., Pokorski, J. K., Commandeur, U., Dubyak, G. R., Steinmetz, N. F., *Acta Biomater.*, 2015, **19**, 166-179.
50. M. Longmire, P. L. Choyke and H. Kobayashi, *Nanomedicine*, 2008, **3**, 703-717.
51. K.-B. G. Scholthof, S. Adkins, H. Czosnek, P. Palukaitis, E. Jacquot, T. Hohn, B. Hohn, K. Saunders, T. Candresse, P. Ahlquist, C. Hemenway and G. D. Foster, *Molecular Plant Pathology*, 2011, **12**, 938-954.
52. B. D. Harrison and T. M. A. Wilson, *Philosophical Transactions of the Royal Society of London. Series B: Biological Sciences*, 1999, **354**, 521-529.
53. A. Klug, *Philosophical Transactions of the Royal Society of London. Series B: Biological Sciences*, 1999, **354**, 531-535.
54. P. Sitasuwan, L. A. Lee, K. Li, H. G. Nguyen and Q. Wang, *Frontiers in Chemistry*, 2014, **2**.
55. T. L. Schlick, Z. Ding, E. W. Kovacs and M. B. Francis, *J. Am. Chem. Soc.*, 2005, **127**, 3718-3723.
56. S. Li, M. Dharmarwardana, R. P. Welch, Y. Ren, C. M. Thompson, R. A. Smaldone and J. J. Gassensmith, *Angew Chem Int Ed Engl*, 2016, **55**, 10691-10696.
57. S. Li, M. Dharmarwardana, R. P. Welch, C. E. Benjamin, A. M. Shamir, S. O. Nielsen and J. J. Gassensmith, *ACS Appl. Mater. Interfaces*, 2018, **10**, 18161-18169.
58. D. Bardelang, K. Banaszak, H. Karoui, A. Rockenbauer, M. Waite, K. Udachin, J. A. Ripmeester, C. I. Ratcliffe, O. Ouari and P. Tordo, *J. Am. Chem. Soc.*, 2009, **131**, 5402-5404.
59. N. Jayaraj, M. Porel, M. F. Ottaviani, M. V. S. N. Maddipatla, A. Modelli, J. P. Da Silva, B. R. Bhogala, B. Captain, S. Jockusch, N. J. Turro and V. Ramamurthy, *Langmuir*, 2009, **25**, 13820-13832.
60. E. Mileo, E. Mezzina, F. Grepioni, G. F. Pedulli and M. Lucarini, *Chemistry - A European Journal*, 2009, **15**, 7859-7862.
61. E. V. Peresyphina, V. P. Fedin, V. Maurel, A. Grand, P. Rey and K. E. Vostrikova, *Chemistry - A European Journal*, 2010, **16**, 12481-12487.
62. Z. Rinkevicius, B. Frecus, N. A. Murugan, O. Vahtras, J. Kongsted and H. Ågren, *J. Chem. Theory Comput.*, 2012, **8**, 257-263.
63. S. Yi, B. Captain, M. F. Ottaviani and A. E. Kaifer, *Langmuir*, 2011, **27**, 5624-5632.
64. S. Kemp, N. J. Wheate, F. H. Stootman and J. R. Aldrich-Wright, *Supramol. Chem.*, 2007, **19**, 475-484.
65. R. N. Dsouza, U. Pischel and W. M. Nau, *Chem. Rev.*, 2011, **111**, 7941-7980.
66. A. Rajca, Y. Wang, M. Boska, J. T. Paletta, A. Olankitwanit, M. A. Swanson, D. G. Mitchell, S. S. Eaton, G. R. Eaton and S. Rajca, *J. Am. Chem. Soc.*, 2012, **134**, 15724-15727.
67. J. T. Paletta, M. Pink, B. Foley, S. Rajca and A. Rajca, *Org. Lett.*, 2012, **14**, 5322-5325.